

Incorporation of the HERG Potassium Channel in a Mercury Supported Lipid Bilayer

Lucia Becucci,^{*,†} Maria V. Carbone,[‡] Tiziana Biagiotti,[‡] Massimo D'Amico,[‡]
Massimo Olivetto,[‡] and Rolando Guidelli[†]

Dipartimento di Chimica, Via della Lastruccia 3, 50019 Sesto Fiorentino (FI), Italy, and Dipartimento di Patologia e Oncologia Sperimentali, Viale G.B. Morgagni 50, 50134 Firenze, Italy

Received: September 18, 2007; In Final Form: November 5, 2007

The HERG potassium channel was incorporated in a mercury-supported tethered bilayer lipid membrane (tBLM) obtained by anchoring a thiolipid monolayer to the mercury surface and by self-assembling a lipid monolayer on top of it from a lipid film spread on the surface of an electrolyte solution. HERG was then incorporated in this tBLM from its micellar solution in Triton X-100, thus avoiding the use of vesicles in the preparation of the tBLM and of proteoliposomes in channel incorporation. The HERG “inward” current following a repolarization step was obtained by subtracting the current recorded upon addition of the specific inhibitor WAY from that recorded prior to this addition. This current was compared with that reported in the literature by the patch-clamp technique.

Introduction

The preparation of rugged lipid bilayers capable of incorporating bulky membrane proteins has been the subject of extensive research. The possibility of using these “biomimetic membranes” for the investigation of the function of membrane proteins and for biosensor applications is of paramount importance. Ion pumps and transporters are commonly investigated on solid supported membranes (SSMs),¹ which consist of a mixed octadecanethiol|phospholipid bilayer anchored to a gold electrode. Proteoliposomes are adsorbed on this bilayer and activated by concentration jumps of a suitable activating substance. On the other hand, ion channels are usually investigated in lipid bilayers suspended in the holes of microporous substrates² or, alternatively, in bilayers tethered to a metal support via a hydrophilic “spacer” (tethered bilayer lipid membranes, tBLMs).¹ Thanks to their particular robustness, tBLMs have potential for biosensor applications. They are obtained by anchoring to the metal surface a “thiolipid”, which consists of a polyethyleneoxy or oligopeptide hydrophilic chain (the spacer) terminated at one end with a sulfhydryl or disulfide group for anchoring to the metal surface and covalently linked at the other end to the polar head of a phospholipid. A lipid monolayer is then self-assembled on top of the thiolipid monolayer, with the polar heads of the lipid turned toward the aqueous solution.

Au-supported tBLMs have been reported to incorporate channel-forming peptides, but also a few bulky proton pumps, such as F₀F₁ ATPase³ and cytochrome *c* oxidase.⁴ In all these cases, the lipid monolayer on top of the thiolipid monolayer was formed from a suspension of vesicles, via vesicle splitting and spreading on the thiolipid monolayer. The ion pump was then incorporated in the tBLM from its aqueous solution in detergent; alternatively, the lipid film was formed by fusion of proteoliposomes containing the integral protein under study. It has been recently reported that vesicles have a low tendency to

fuse on hydrophobic surfaces, such as that exposed to the aqueous solution by a thiolipid monolayer;^{5,6} rather, they are adsorbed or partially fused. The outermost portion of the lipid bilayer enclosing partially fused vesicles may incorporate proteins from their detergent solutions, since it is interposed between two aqueous phases. An analogous state is attained with proteoliposomes partially fused on the thiolipid monolayer from their suspensions. The functional activity of the above proton pumps may well be successfully verified even with vesicles or proteoliposomes partially fused on a thiolipid monolayer, without the necessity of forming a well-behaved tBLM. In fact, their activation causes an increase in the proton concentration in contact with the thiolipid monolayer (in the case of F₀F₁ ATPase activated by ATP³) or its decrease (in the case of cytochrome *c* oxidase activated by ferrocyanide⁴). In view of the relative permeability of leaky thiolipid monolayers to protons, this may cause an increase or a decrease, respectively, in the proton electroreduction current on gold, as was actually observed.

More recently, Naumann et al. have synthesized and characterized a thiolipid, called DPTL, which consists of a hydrophilic tetraethyleneoxy (TEO) chain covalently linked to a lipoic acid residue for anchoring to the metal at one end, and bound via ether linkages to two phytanyl chains at the other end.⁷ The use of this thiolipid in place of the oligopeptide-based thiolipids adopted with the aforementioned proton pumps has notably increased the resistance of the resulting Au-supported tBLMs, drastically reducing pinholes and other defects that may provide preferential pathways for electron and ion transport across the lipid bilayer. Valinomycin^{7b} and the channel-forming peptides gramicidin and melittin^{7d} have been incorporated in Au-supported DPTL|phospholipid tBLMs, and their functional activity has been verified. However, solid metals such as Au block the lateral movement of the thiolipid molecules, which are linked to the surface atoms of the metal by covalent bonds. It is, therefore, quite difficult to succeed in incorporating bulky channel-forming proteins in Au-supported tBLMs. Moreover, channel-forming proteins must span the whole tBLM, including

* Corresponding author. Telephone: (+37) 055-457-309. Fax: (+39) 055-457-3385. E-mail: lucia.becucci@unifi.it.

[†] Dipartimento di Chimica.

[‡] Dipartimento di Patologia e Oncologia Sperimentali.

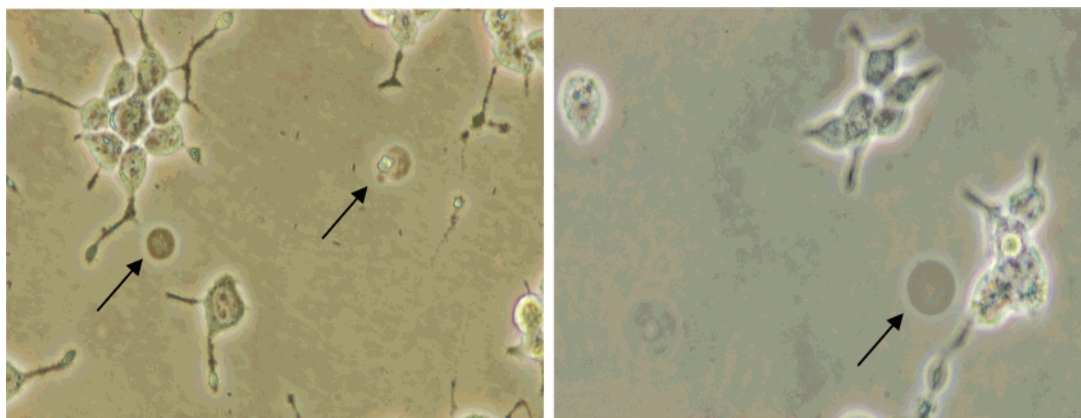


Figure 1. Contrast-phase images of vesicles produced by stimulated HEK 293 clone 5 (arrows); 40 \times .

the thiolipid monolayer, in order to translocate ions into the hydrophilic TEO moiety and to give rise to a resulting capacitive current.

Two of us have used DPTL/lipid tBLMs supported by mercury to incorporate the ion carrier valinomycin,⁸ the channel-forming peptides melittin⁹ and gramicidin,¹⁰ and the channel-forming protein porin from *Escherichia coli*.¹¹ Thanks to its liquid nature, mercury provides a defect-free surface to the self-assembling film, and imparts a high fluidity to the tBLM by allowing the lateral movement of the thiolipid molecules anchored to its surface. The self-assembly of a lipid monolayer on top of the thiolipid-coated mercury is carried out by immersing the mercury drop in an aqueous electrolyte on whose surface a lipid film has been previously spread, thus avoiding the use of vesicles. The present note describes the incorporation of the HERG potassium channel in this mercury-supported tBLM.

Experimental Methods

Diphytanoylphosphatidylcholine (PC) was purchased from Avanti Polar Lipids (Birmingham, AL), sphingomyelin (SM) was purchased from Lipid Products (Surrey, U.K.), and cholesterol (Chol) was purchased from Sigma. The 2,3-di-*O*-phytanoyl-*sn*-glycerol-1-tetraethylene glycol-DL- α -lipoic acid ester lipid (DPTL) was kindly provided by Prof. Adrian Schwan (Chemistry Department, Guelph University, Canada).

The HERG protein was extracted with 1% v/v Triton X-100 from vesicles produced by ad hoc stimulated human embryonic kidney (HEK-293) cells, transfected with *herg1* cDNA, and highly expressing a HERG current endowed with all the biophysical and pharmacological properties described in the literature for the HERG channel. The HEK-293 cells were grown in DMEM supplemented with 10% fetal calf serum (FCS) (Hyclone). They were transfected with *herg1* cDNA cloned into *HindIII/BamHI* sites of the pCDNA3.1 vector by the calcium phosphate method, obtaining the HEK-293 clone 5. The clone was grown with supplement of Geneticin (G-418, 50 mg/mL). Membrane fragments were isolated from culture media by ultracentrifugation.¹² Briefly, samples of media were removed from subconfluent cell cultures, centrifuged at 27000g for 15 min to remove cell debris and concentrated using dialysis membranes (cutoff 12–14 000 Da). The concentrated material was centrifuged at 150000g and the pellet was washed and resuspended in 1 mM PBS, pH 7.4. Control and transfected HEK-293 cells were also stimulated (see Figure 1) to produce membrane fragments, by exposition to 25 mM formaldehyde/2 mM dithiothreitol in phosphate-buffered saline (0.75 mM CaCl₂ and 0.5 mM MgCl₂). The HERG protein was extracted from

the purified vesicles by a treatment with 1% v/v Triton X-100 for 20 min, followed by centrifugation to separate the HERG solution from debris. The HERG protein content in the supernatant was verified by immunoblotting analysis using an anti-HERG channel antibody (Alomone, 1:400).

HERG is completely soluble in Triton X-100 even at concentrations as low as 0.1%;¹³ this avoids significant aggregation of the protein due to misfolding produced by resistance to detergent extraction. Another cause of protein aggregation is the presence of reactive oxygen species, such as those formed by oxidation of unsaturated lipids or other endogenous species.¹⁴ To eliminate this possible source of aggregation, only saturated lipids were employed for the preparation of the tBLM and all measurements were carried out in solutions deaerated with nitrogen gas (see below).

SM and Chol stock solutions were prepared by dissolving these lipids in chloroform. PC solutions were prepared by diluting proper amounts of its stock solution with pentane. Lipid mixtures were obtained by diluting proper amounts of each lipid stock solution with pentane to obtain the composition PC:SM:Chol (59:15:26). Solutions of 0.2 mg/mL DPTL in ethanol were prepared from a 2 mg/mL solution of DPTL in ethanol. Stock solutions of this thiolipid were stored at -18°C . All measurements were carried out in aqueous 0.1 M KCl. Use was made of a homemade hanging mercury drop electrode (HMDE), described elsewhere.¹⁵ A homemade glass capillary with a finely tapered tip, about 1 mm in outer diameter, was employed. The capillary and the mercury reservoir were thermostated at $25 \pm 0.1^{\circ}\text{C}$ in a water-jacketed box to avoid any changes in drop area due to a change in temperature. A glass electrolysis cell containing the aqueous solution and a small glass vessel containing the ethanol solution of the thiolipid were placed on a movable support inside the box. The HMDE and the support were moved vertically and horizontally, respectively, by means of two oleodynamic systems that ensured the complete absence of vibrations. Chronocoulometric and ac voltammetric measurements were carried out with an Autolab PGSTAT12 (Echo Chemie) instrument supplied with a FRA2 module for impedance measurements, a SCAN-GEN scan generator, and GPES 4.9005 Beta software. Potentials were measured versus a Ag|AgCl electrode immersed in the 0.1 M KCl working solution, but are referred to a saturated calomel electrode (SCE).

Monolayers of DPTL were self-assembled on the HMDE by keeping the mercury drop immersed in the small vessel containing the thiolipid solution for 20 min. In the meantime, the aqueous solution in the glass cell was deaerated with nitrogen, the PC:SM:Chol (59:15:26) lipid mixture in pentane was then spread on its surface in an amount corresponding to

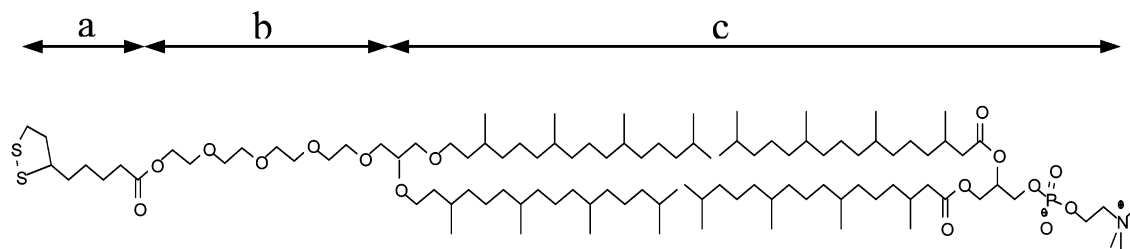


Figure 2. Schematic picture of the different substructures of a tBLM, with the primary structure of the DPTL thiolipid in contact with that of a diphytanoylphosphatidylcholine molecule. (a) Lipoic acid residue, ~ 0.64 nm in length; (b) tetraethyleneoxy moiety, ~ 1.6 nm in length; (c) lipid bilayer moiety, ~ 5.0 nm in length.

five to six lipid monolayers, and the pentane was allowed to evaporate. This lipid composition was chosen because it is close to that of the membrane of an average mammalian cell. Using the oleodynamic system, the DPTL-coated HMDE was then extracted from the vessel, washed with ethanol to remove the excess of adsorbed thiolipid, and kept in a nitrogen atmosphere for the time strictly necessary to allow the solvent to evaporate. Immediately afterward, the electrolysis cell containing the aqueous solution with the lipid film on its surface, which was constantly kept under a nitrogen blanket, was brought below the HMDE and the latter was lowered so as to immerse it in the aqueous solution across the lipid film; this procedure causes a lipid monolayer to self-assemble on top of the DPTL monolayer, giving rise to a lipid bilayer interposed between the hydrophilic TEO moiety of the thiolipid and the aqueous solution. The applied potential was then repeatedly scanned over a potential range from -0.200 to -1.200 V while continuously monitoring the curve of the quadrature component, Y'' , of the electrode admittance at 75 Hz against the applied potential, E , using ac voltammetry, until a stable Y'' versus E curve was attained. The resulting (DPTL/lipid)-coated mercury had a capacity of $0.55\text{--}0.65 \mu\text{F cm}^{-2}$ and a resistance of $5\text{--}10 \text{ M}\Omega \text{ cm}^2$.

Results and Discussion

The HERG K^+ channel is composed of four identical subunits, each containing six transmembrane-spanning domains. It may exist in one of three basic conformations: closed (C), open (O), and inactive (I).¹⁶ Starting from the resting potential, a positive potential step (depolarization) causes the channel to pass relatively slowly from the C to the O conformation, but very rapidly from the O to the I conformation; consequently, the resulting outward current lasts for about 1 ms and is very low. A subsequent potential step to a value more negative than the reversal potential for K^+ (hyperpolarization) causes a very fast passage from the I to the O conformation and a relatively slow passage from the O to the C conformation. Consequently, the inward current following the latter passage lasts for more than 100 ms and is much higher than the outward current.

To measure the inward current following the passage from the O to the C conformation of HERG channels incorporated in the tBLM, the potential difference across the lipid bilayer moiety of the tBLM (namely, the transmembrane potential ϕ_2) must first be estimated. An electrochemical impedance spectroscopic analysis of the tBLM indicates that it can be regarded as consisting of three substructures with different dielectric properties and relaxation times: the lipoic acid residue, the TEO moiety, and the lipid bilayer moiety (see Figure 2). Their differential capacities amount to, in order, $C_0 = 4 \mu\text{F cm}^{-2}$, $C_1 = 7 \mu\text{F cm}^{-2}$, and $C_2 = 1 \mu\text{F cm}^{-2}$.⁸ Several pieces of experimental evidence indicate that the absolute potential difference, $\Delta\phi$, across the whole mercury|(aqueous solution)

interface is more positive than the applied potential E measured vs a saturated calomel electrode (SCE) by about 0.250 V: $\Delta\phi = E/\text{SCE} + 0.250$ V.¹⁷ Moreover, independent measurements point to a surface dipole potential, χ_1 , of the TEO moiety of about -0.250 V, negative toward the electrode surface.¹⁸ If no ions are present in the TEO moiety, $\Delta\phi$ is given by

$$\Delta\phi = E/\text{SCE} + 0.250 \text{ V} = \sigma_M/C_0 + (\sigma_M/C_1 + \chi_1) + \sigma_M/C_2 \equiv \phi_0 + \phi_1 + \phi_2 \quad (1)$$

where σ_M is the charge density on the metal, and the three terms on the right-hand side of eq 1 are, in order, the potential differences across the lipoic acid residue, the TEO moiety, and the lipid bilayer. By extracting σ_M from eq 1 and replacing its expression in that of the transmembrane potential ϕ_2 , we obtain

$$\phi_2 = \frac{E/\text{SCE} + 0.250 \text{ V} - \chi_1}{(C_0^{-1} + C_1^{-1} + C_2^{-1})C_2} \quad (2)$$

Using the above values of C_0 , C_1 , C_2 , and χ_1 in eq 2, the transmembrane potential in the absence of ionic charges in the TEO moiety is approximately given by $\phi_2 = 0.72(E/\text{SCE} + 0.500 \text{ V})$.

Before adding the Triton X-100 solubilized HERG to the 0.1 M KCl working solution, the stability of the tBLM in the presence of Triton X-100 was verified by recording its electrochemical impedance spectrum over the bias potential range from -0.300 to -1.000 V, by 50 mV steps, upon varying the frequency of a 10 mV peak-to-peak ac signal over the range from 1×10^{-2} to 1×10^5 Hz at each bias potential; addition of $1 \times 10^{-2}\%$ v/v Triton X-100 to the 0.1 M KCl solution had no effect on the spectrum over the whole potential range investigated. Subsequently, $20 \mu\text{L}$ of HERG solution in 1% v/v Triton X-100 was added to 5 mL of 0.1 M KCl in the electrolysis cell. This dilution brought Triton X-100 below its critical micelle concentration (cmc), causing the release of the free protein and its incorporation in the preformed tBLM. The incorporation was favored by superimposing 10 mV peak-to-peak ac signals of frequency ranging from 0.1 to 10^5 Hz on a bias potential varying gradually from -0.3 to -0.8 V by 100 mV steps. The progress in the incorporation was followed by carrying out potential steps, up to stabilization. The stability of the tBLM in Triton X-100 did not require its removal from the working solution. After attaining stabilization and recording the current and charge transients, biobeads were added to the electrolysis cell in order to sequester Triton X-100, and the recordings were repeated. No effect of the biobeads was observed; this indicates that bringing Triton X-100 below its cmc was sufficient to release the protein completely.

After incorporating HERG in the tBLM from its solution in detergent, a series of potential steps was carried out in 0.1 M KCl from -0.300 to -0.720 V/SCE, with a rest time of 2 min

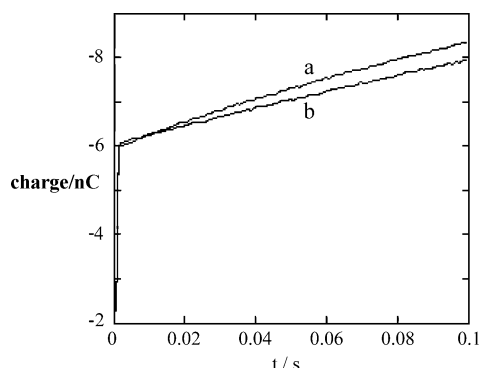


Figure 3. Charge vs time t curves following a potential step from -0.300 to -0.720 V/SCE at a tBLM incorporating HERG in 0.1 M KCl, both before (a) and after addition of $5 \mu\text{M}$ WAY (b).

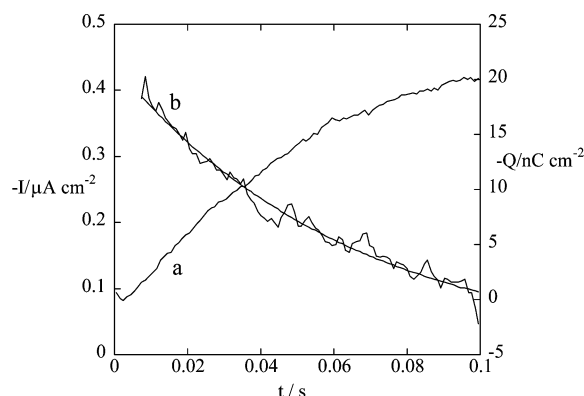


Figure 4. Charge Q (a) and current I (b) ascribable to HERG activation against time t , obtained by stepping the potential from -0.300 to -0.720 V/SCE at a tBLM incorporating HERG in 0.1 M KCl. The smooth curve is a fit of a single-exponential function to curve b.

at -0.300 V/SCE before each step, and the current and charge following each step were recorded simultaneously against time. This E step corresponds to a potential step from $+145$ to -158 mV across the lipid bilayer moiety of the tBLM, as measured on the TEO side of the bilayer with respect to the aqueous phase.

Curve a in Figure 3 shows the mean of 10 successive charge records. In practice, these records were indistinguishable from each other in the time scale of Figure 3, and their mean was carried out only to reduce the noise. The abruptly rising section of curve a, which lasts a few milliseconds, is due to the rapid charging of the electrode surface. This is followed by a slow increase of charge, due to the high, but noninfinite resistance of the tBLM, and to the flow of potassium ions along the HERG channels. To single out the contribution from the HERG channels, a specific inhibitor of HERG, WAY,¹⁹ was added to the solution at $5 \mu\text{M}$ concentration. After attaining signal stabilization, which required about 5 min, a new series of charge and current records was carried out, by the same protocol adopted before the WAY addition. Curve b in Figure 3 shows a mean of 10 charge records. Subtracting curve b from curve a yields the curve of the charge Q against time ascribable to the activation of the HERG channels. This is shown in Figure 4, curve a, together with the corresponding curve of the current I against time (curve b), obtained by the same procedure. The smooth curve is a fit of a single-exponential function to curve b, which yields a time constant of 65 ms. This should be compared with the time constants for the HERG channel obtained by patch clamping oocytes at different repolarization potentials.²⁰ These time constants decrease from 80 to 20 ms with a decrease in the repolarization potential from -90 to -140 mV, a 65 ms value being attained in the proximity of -100

mV. The discrepancy between the latter transmembrane potential and that, -158 mV, yielding the same time constant in the present measurements is to be ascribed to the different experimental conditions. Thus, for instance, the small thickness of the TEO moiety is such that a modest accumulation of positive ions into this hydrophilic spacer causes a positive shift in the transmembrane potential ϕ_2 , which, in the case of Figure 3, can be estimated at about 20 mV.

The exact distribution of the incorporated HERG channels between the two possible orientations is not known. As a rule, integral proteins are inserted through the hydrophobic domain of a membrane with their more hydrophobic moiety first.²¹ In the present case, one must also consider that the small thickness of the hydrophilic TEO moiety (~ 1.6 nm), in comparison with the semi-infinite aqueous phase, favors the orientation with the bulkier extramembrane domain directed toward the aqueous phase. A number of potassium channels, such as that from *Streptomyces lividans*, have an extracellular domain somewhat bulkier than the intracellular one.²² The HERG channel has two intracellular domains (the N- and C-terminals) and an S5-P linker, a P loop, and a P-S6 linker around the outer mouth of the channel. With respect to other K^+ channels, such as the Shaker channel, HERG has a more flexible outer mouth and a much longer S5-P linker, whose central segment may form an α -helix.²³ We may, therefore, tentatively hypothesize a preferential orientation of HERG with the extracellular side turned toward the aqueous phase.

At any rate, only the channels with the latter orientation can move K^+ ions across the lipid bilayer. At the initial potential of -0.300 V/SCE, these channels experience a transmembrane potential of about $+145$ mV and are in the I conformation; the subsequent negative potential step hyperpolarizes the membrane, giving rise to a relatively large inward current that moves K^+ ions from the aqueous phase to the TEO moiety. This ionic flux tends to create a potential difference positive toward the metal. At the constant final potential of -0.720 V/SCE, this potential difference is almost instantaneously compensated for by an equal and opposite potential difference produced by a flow of electrons along the external circuit, recorded as a negative capacitive current. Conversely, any HERG channels incorporated with the intracellular side turned toward the aqueous phase experience a transmembrane potential of -145 mV at the initial applied potential of -0.300 V/SCE. They are, therefore, in the C conformation; the subsequent potential step to -0.720 V/SCE, corresponding to a transmembrane potential of $+158$ mV, depolarizes the membrane causing them to pass to the I conformation, via the O one. The resulting "outward" current from the aqueous phase to the TEO moiety is very small and lasts for about 1 ms. It should be noted that the procedure used to prepare the tBLM excludes the presence of K^+ and Cl^- ions within the TEO moiety prior to the addition of HERG, and that the repeated potential steps carried out during the measurements inject only a very small amount of K^+ ions into this hydrophilic spacer.

The HERG inward current is due to a flux of K^+ ions along the pores formed by aggregation of four identical subunits. Quite probably, they were formed by spontaneous aggregation of the single subunits in the lipid bilayer, upon their release by the detergent and their incorporation. The single channel current of HERG is on the order of 5 pA. Consequently, the density of HERG tetramers responsible for the initial current in Figure 4 may be roughly estimated at 10^5 molecules cm^{-2} .

A few attempts to use pure diphytanoylphosphatidylcholine in place of the PC:SM:Chol (59:15:26) lipid mixture were

unsuccessful, probably because of a smaller incorporation of HERG and of a resulting inward current that was comparable with the electrical noise. The electrical noise prevented us from carrying out measurements at different HERG concentrations even with the PC:SM:Chol (59:15:26) lipid mixture. In fact, the results reported herein were obtained with a relatively high HERG concentration in solution, when a further increase in concentration had already a negligible effect on the HERG inward current. On the other hand, lower HERG concentrations in solution yielded inward currents that were too low to be accurately measured.

Attempts were also made to incorporate HERG by spontaneous splitting and spreading of HERG containing vesicles on a Hg-supported DPTL monolayer. No detectable inward current ascribable to the HERG activation was obtained by this procedure. This indicates that vesicles have no tendency to fuse on the hydrophobic surface of the DPTL monolayer. The HERG channels present in any adsorbed or partially fused vesicles cannot be activated by potential steps, because the largest fraction of the resulting ohmic drop is localized in the DPTL monolayer.

Conclusions

The HERG channel was successfully incorporated in a mercury-supported tBLM in a functionally active state, without having recourse to vesicles or proteoliposomes. This confirms the potential of mercury-supported tBLMs in incorporating bulky channel-forming membrane proteins. Mercury can be easily electrodeposited on Pt²⁴ or Ir²⁵ microelectrodes, and can also be coated with DPTL/lipid bilayers exhibiting resistances of several gigohms. The preparation of these biomimetic micromembranes for single channel recordings is in progress. This will open the way to the fabrication of arrays of micromembranes very adaptable for high throughput screening technologies.

Acknowledgment. Thanks are due to Ente Cassa di Risparmio di Firenze for financial support through the PROMELAB project.

References and Notes

- (1) Guidelli, R.; Aloisi, G.; Becucci, L.; Dolfi, A.; Moncelli, M. R.; Tadini Buoninsegni, F. *J. Electroanal. Chem.* **2001**, *504*, 1–28, and references therein.
- (2) (a) Bavero, G.; Campanella, L.; Cavallo, S.; D'Annibale, A.; Perrella, M.; Mattei, E.; Ferri, T. *J. Am. Chem. Soc.* **2005**, *127*, 8103–8111. (b) Matsuno, N.; Murawsky, M.; Ridgeway, J.; Cuppoletti, J. *Biochim. Biophys. Acta* **2004**, *1665*, 184–190. (c) Römer, W.; Steinem, C. *Biophys. J.* **2004**, *86*, 955–965. (d) Horn, C.; Steinem, C. *Biophys. J.* **2005**, *89*, 1046–1054.
- (3) (a) Naumann, R.; Jonczyk, A.; Hampel, C.; Ringsdorf, H.; Knoll, W.; Bunjes, N.; Gräber, P. *Bioelectrochem. Bioenerg.* **1997**, *42*, 241–247. (b) Naumann, R.; Baumgart, T.; Gräber, P.; Jonczyk, A.; Offenhäusser, A.; Knoll, W. *Biosens. Bioelectron.* **2002**, *17*, 25–34.
- (4) Naumann, R.; Schmidt, E. K.; Jonczyk, A.; Fendler, K.; Kadenbach, B.; Liebermann, T.; Offenhäusser, A.; Knoll, W. *Biosens. Bioelectron.* **1999**, *14*, 651–662.
- (5) Baumgart, T.; Kreiter, M.; Lauer, H.; Naumann, R.; Jung, G.; Jonczyk, A.; Offenhäusser, A.; Knoll, W. *J. Colloid Interface Sci.* **2003**, *258*, 298–309.
- (6) Zebrowska, A.; Krysinski, P. *Langmuir* **2004**, *20*, 11127–11133.
- (7) (a) Schiller, S. M.; Naumann, R.; Lovejoy, K.; Kunz, H.; Knoll, W. *Angew. Chem., Int. Ed.* **2003**, *42*, 208–211. (b) Naumann, R.; Walz, D.; Schiller, S. M.; Knoll, W. *J. Electroanal. Chem.* **2003**, *550–551*, 241–252. (c) Naumann, R.; Schiller, S. M.; Giess, F.; Grohe, B.; Hartman, K. B.; Kärcher, I.; Köper, I.; Lübken, J.; Vasilev, K.; Knoll, W. *Langmuir* **2003**, *19*, 5435–5443. (d) He, L.; Robertson, J. W. F.; Li, J.; Kärcher, I.; Schiller, S. M.; Knoll, W.; Naumann, R. *Langmuir* **2005**, *21*, 11666–11672. (e) Robelek, R.; Lemker, E. S.; Wiltzsch, B.; Kirste, V.; Naumann, R.; Oesterheld, D.; Sinner, E.-K. *Angew. Chem., Int. Ed.* **2007**, *46*, 605–608.
- (8) Becucci, L.; Moncelli, M. R.; Naumann, R.; Guidelli, R. *J. Am. Chem. Soc.* **2005**, *127*, 13316–13323.
- (9) (a) Becucci, L.; Romero León, R.; Moncelli, M. R.; Rovero, P.; Guidelli, R. *Langmuir* **2006**, *22*, 6644–6650. (b) Becucci, L.; Guidelli, R. *Langmuir* **2007**, *23*, 5601–5608.
- (10) Becucci, L.; Santucci, A.; Guidelli, R. *J. Phys. Chem. B* **2007**, *111*, 9814–9820.
- (11) Becucci, L.; Moncelli, M. R.; Guidelli, R. *Langmuir* **2006**, *22*, 1341–1346.
- (12) Rigaud, J. L.; Levy, D. *Methods Enzymol.* **2003**, *372*, 65–86.
- (13) Gong, Q.; Jones, M. A.; Zhou, Z. *J. Biol. Chem.* **2006**, *281*, 4069–4074.
- (14) Zhang, Y.; Xiao, J.; Wang, H.; Luo, X.; Wang, J.; Villeneuve, L. R.; Zhang, H.; Bai, Y.; Yang, B.; Wang, Z. *Am. J. Physiol. Heart Circ. Physiol.* **2006**, *291*, 1446–1455.
- (15) Moncelli, M. R.; Becucci, L. *J. Electroanal. Chem.* **1997**, *433*, 91–96.
- (16) (a) Trudeau, M. C.; Warmke, J. W.; Ganetzky, B.; Robertson, G. A. *Science* **1995**, *269*, 92–95. (b) Arcangeli, A.; Bianchi, L.; Becchetti, A.; Faravelli, L.; Coronello, M.; Mini, E.; Olivotto, M.; Wanke, E. *J. Physiol.* **1995**, *489.2*, 455–471. (c) Smith, P. L.; Baukrowitz, T.; Yellen, G. *Nature* **1996**, *379*, 833–836.
- (17) Becucci, L.; Moncelli, M. R.; Guidelli, R. *Langmuir* **2003**, *19*, 3386–3392.
- (18) Moncelli, M. R.; Becucci, L.; Schiller, S. M. *Bioelectrochemistry* **2004**, *63*, 161–167.
- (19) D'Amico, M.; Biagiotti, T.; Fontana, L.; Restano-Cassulini, R.; Lasagna, N.; Arcangeli, A.; Wanke, M.; Olivotto, M. *Biochem. Biophys. Res. Commun.* **2003**, *302*, 101–108.
- (20) Morais Cabral, J. H.; Lee, A.; Cohen, S. L.; Chait, B. T.; Li, M.; Mackinnon, R. *Cell* **1998**, *95*, 649–655.
- (21) Eytan, G. D. *Biochim. Biophys. Acta* **1982**, *694*, 185–202.
- (22) Doyle, D. A.; Morais Cabral, J.; Pfuetzner, R. A.; Kuo, A.; Gulbis, J. M.; Cohen, S. L.; Chait, B. T.; MacKinnon, R. *Science* **1998**, *280*, 69–77.
- (23) Zhang, M.; Liu, J.; Tseng, G.-N. *J. Gen. Physiol.* **2004**, *124*, 703–718.
- (24) Baldo, M. A.; Bragato, C.; Daniele, S. *Electroanalysis* **2003**, *15*, 621–628.
- (25) Silva, P. R. M.; El Khakani, M. A.; Le Droff, B.; Chaker, M.; Vijh, A. K. *Sens. Actuators, B* **1999**, *60*, 161–167.